# Auxin is not asymmetrically distributed in initiating Arabidopsis leaves

**Neha Bhatia[1] and Marcus G. Heisler[1*]**

**Affiliations**

[1]School of Life and Environmental Sciences, University of Sydney, NSW, Australia

*Author for correspondence: Marcus G Heisler (marcus.heisler@sydney.edu.au)

**Abstract**

It has been proposed that asymmetric auxin levels within initiating leaves help establish leaf polarity, based in part on observations of the DII auxin sensor. Here we show that the mDII control sensor also exhibits an asymmetry and that according to the ratio-metric auxin sensor R2D2, no obvious asymmetry in auxin exists. Together with other recent findings, our results argue against the importance of auxin asymmetry in establishing leaf polarity.

## Results and Discussion

The leaves of seed plants are usually flat with distinct cell types making up their dorsal (upper) and ventral (lower) tissues. A fundamental question in plant development is how this dorsal-ventral polarity is first specified. Studies based on wounding experiments have suggested the presence of an inductive signal originating from the meristem that promotes dorsal identity in the adaxial (adjacent to the meristem) tissues of the leaf primordium[1,2]. However more recently, it was found that exogenous application of the plant hormone auxin to tomato leaf primordia resulted in the formation of radialized leaves that appeared ventrilized. Hence, relatively high levels of auxin are proposed to promote ventral or inhibit dorsal leaf cell fate[3]. Extending these conclusions, it was also proposed that an asymmetry in the auxin distribution across the leaf adaxial-abaxial axis at leaf initiation acts to help specify leaf polarity during regular development[3]. A critical piece of evidence supporting this latter proposal is that an auxin sensor, the DII[4,5] indicates low levels of auxin in adaxial leaf tissues compared to abaxial tissues at leaf initiation[3]. Hence asymmetries in auxin concentrations between the adaxial and abaxial leaf tissues, as a result of PIN1 mediated auxin transport, are proposed to help establish leaf polarity[3]. Building on this conclusion, a more recent study proposed that low levels of auxin in adaxial

tissues are necessary to restrict the expression of the WOX1 and PRS genes to the middle domain, since auxin promotes their expression[6]. Finally, the reported asymmetry in auxin has also been linked to asymmetries in the mechanical properties of leaf tissues and their morphogenesis[7].

Despite these studies, reason to reassess the role of any asymmetry in auxin in specifying leaf polarity has arisen due to the recent finding that the expression patterns of genes involved in leaf dorsoventrality are already patterned in meristem tissues where leaves originate, with little change occurring to their expression during organ initiation. Hence leaf polarity appears pre-patterned [8]. Furthermore, rather than compromise dorsal cell fate, auxin was found to promote dorsal cell fate by maintaining Class III HD-ZIP expression and repressing KAN1 expression in the adaxial cells of organ primordia[8], which is the opposite of what would be expected according to the auxin asymmetry hypothesis. In addition, Caggiano et al. (2017) also found that exogenous auxin application to young leaf primordia did not influence the spatial pattern of WOX1 and PRS, only the intensity of expression[8]. This also conflicts with the proposal that low levels of auxin are required in adaxial leaf tissues to prevent ectopic WOX1 and PRS expression as previously proposed[6].

Given the concerns listed above, we decided to examine the distribution of auxin during leaf initiation using not only by the DII sensor assessed in previous studies but also, by looking more closely at the expression pattern of the non-auxin degradable mDII auxin sensor control[4] as well as the ratiometric R2D2 auxin sensor[9]. We initially focused on the first two leaves three and four days after stratification (DAS), when these leaves are initiating as well as a day later as they begin to elongate and included the PIN1-GFP marker in our analysis to correlate auxin levels with PIN1 expression and polarity. At 3DAS, the expression patterns of REV and KAN1 are already polar within such primordia, although the FIL expression domain at this stage of development is still being refined[8]. Also at this stage, PIN1 is polarized towards the distal tip of leaf primordia but has reversed polarity away from the primordia, towards the meristem, in cells adjacent to the primordia on the adaxial side. According to the ratio-metric auxin sensor R2D2, auxin concentrations were relatively low in adaxial cells of the primordia but also low in abaxial and lateral regions proximally (Fig1-a and d; Fig.S1). High levels of auxin were only found in more distal regions towards

67 the tip of the primordia, matching the overall pattern of signal from PIN1-GFP. No
68 obvious asymmetry in signal between the adaxial and abaxial sides of the primordia
69 was observed. This same overall pattern of signal was found in 16 out of 18 leaves
70 that were examined. At 4DAS, the auxin distribution according to the R2D2 sensor
71 was more uniform although higher levels of auxin appeared associated with the
72 vasculature, again correlating with PIN1 expression (n=12/12 leaves) (Fig. 1 g and j).
73
74 As our results using the R2D2 auxin sensor indicate a different auxin distribution
75 compared to that reported previously using the DII marker [3], we next re-examined the
76 pattern of DII auxin sensor expression at the same developmental stages. In contrast
77 to the R2D2 pattern, the DII pattern showed an asymmetry of expression in leaf
78 primordia at 3 DAS, indicating relatively low auxin levels in adaxial primordium
79 cells, as found previously. DII signal appeared strongest in the adaxial epidermis but
80 was also stronger in the adaxial sub-epidermal cell layer compared to abaxial
81 epidermal and sub-epidermal cell layers (Fig.1- b, e, h and Fig. S2) (n=18/18 leaves).
82 One day later, although DII signal was still higher in the adaxial cells of the
83 primordia, it started to show a relatively increased expression in the abaxial sub-
84 epidermal layers as well compared to earlier stage (n=13/14 leaves) (Fig1-k). Overall
85 our results using the DII marker are similar to those obtained previously and
86 consistent with the proposal that there are low levels of auxin in the adaxial regions of
87 leaf primordia, in contrast to our results using the R2D2 sensor. Given this
88 discrepancy, we next examined the expression of the mDII sensor which is driven by
89 the same 35S promoter as the DII sensor but is not auxin sensitive. Surprisingly we
90 found that, like the DII results, expression of the mDII marker was also higher in the
91 adaxial cells of the primordia (n= 16/16 leaves) (Fig.1-c,f,i and Fig.S3). The pattern
92 appeared almost identical to the pattern found using the DII marker except that the
93 mDII marker also showed high levels of expression in the shoot meristem whereas the
94 DII sensor did not (compare Fig1-b,c; Fig S2 a-h and Fig S3 a-f ). The similarity of
95 expression between DII and mDII was also apparent at 4DAS when the leaves had
96 started to elongate (Fig.1-l) (n=14/14 leaves). To verify the auxin sensitivity of the
97 sensors used we imaged seedlings before and after treatment with 5mM NAA and
98 found a strong decrease in DII expression compared to mDII and an increase in the
99 ratio of VENUS compared to tdTomato signal for the R2D2 sensor, consistent with an
100 increase in auxin levels (Figure S4).

101

102 All together these results indicate that the asymmetry in expression found previously
103 for the DII auxin sensor in very young leaf primordia[3] is not due to an asymmetry in
104 auxin levels but rather, likely due to differences in transcription driven by the 35S
105 promoter used to drive both DII and mDII in adaxial compared to abaxial leaf tissues.
106 We note that although a single section showing control expression of mDII in older
107 leaves was cited by Guan et al., (2017)[10], our results show that this information was
108 not adequate for assessing similarities and differences between DII and mDII at early
109 developmental stages. To check whether adaxial expression in leaf primordia is a
110 characteristic common to other reporters driven by the 35S promoter, we also
111 examined the expression of 35S::H2B-mRFP1 and 35S::EGFP-LTI6b which had
112 previously been combined into the same plant line by crossing[11]. Surprisingly the
113 expression patterns for these markers were not only different to the mDII marker but
114 also different to each other with the H2B marker showing stronger expression in the
115 adaxial and abaxial epidermis and the LTI6b marker showing a more uniform pattern
116 (Fig. S5). These results reveal that even when the same promoter is utilized to drive
117 FP (fluorescent protein) expression, distinct differences in intensity patterns can occur
118 *in planta*. This may be due to differences in the position of T-DNA insertion in the
119 genome or differences in the surrounding DNA of the vector used. All together then,
120 our results highlight the importance of using ratio-metric sensors for *in vivo*
121 measurements since otherwise it is difficult to adequately control for differences in
122 signal intensity due to promoter activity or other confounding factors. Finally, while
123 the R2D2 marker utilizes a single transgene to express two distinct FPs from two
124 identical promoters[9], a potentially improved approach to assess auxin levels *in vivo*
125 may be to utilize a single promoter to drive the auxin-dependent degradation domain
126 II from Aux/IAA proteins linked to a tandem fusion of fast and slowly folding FP
127 variants, such as VENUS and mCherry. Such an approach can enable a more direct
128 readout of protein degradation rates[12,13] and therefore potentially improve
129 measurements of relative auxin concentration.

130

131 While our findings are inconsistent with the proposal that asymmetries in the auxin
132 distribution influence leaf polarity[3], pattern WOX/PRS gene expression [6] or regulate
133 tissue mechanics[7], they also leave other observations unexplained. In particular, to
134 understand the apparent ventrilization of leaf primordia in tomato in response to

135 exogenous auxin[3] will require further work in assessing how auxin distribution
136 patterns change in response to exogenous treatments and how auxin is distributed
137 during regular development in tomato, preferentially using a ratio-metric auxin sensor
138 such as R2D2.
139
140 **Methods**
141 **Plant material and growth conditions.**
142 Seeds of the plants expressing *p35S::DII-VENUS* and *p35S::mDII-VENUS*
143 transgenes (*Columbia* ecotype) were obtained from Dr. Teva Vernoux [4]. An
144 independent batch of seeds expressing *p35S::mDII-VENUS* transgenes (*Columbia*
145 ecotype) was also obtained from NASC (Arabidopsis stock center, NASC ID:
146 N799174) for analysis. R2D2 reporter line carrying *pPIN1::PIN1GFP* transgene
147 (*Landsberg* ecotype) has been described previously[9,14]. Seeds were germinated and
148 grown on GM medium (pH-7 with 1M KOH) containing 1% sucrose, 1X Murashige
149 and Skoog salts (Sigma M5524), MES 2-(MN-morpholino)- ethane sulfonic acid
150 (Sigma M2933), 0.8 % Bacto Agar (Difco), 1% MS vitamins (Sigma M3900) in long
151 day conditions.
152
153 **Confocal imaging and data analysis**
154 Seedlings aged 3DAS (days after stratification) and 4DAS were dissected as
155 described previously[14]. Dissected seedlings were then oriented appropriately to obtain
156 a view of the young leaves either from above or from the side. Seedlings were imaged
157 live, on a Leica TCS-SP5 upright confocal laser scanning microscope with hybrid
158 detectors (HyDs) using a 25X water objective (N.A 0.95). VENUS was imaged using
159 argon laser (excitation wavelength 514nm) while tdTomato was imaged using a white
160 light laser (excitation wavelength 561 nm). Z-stacks were acquired in a 512x512 pixel
161 format with section spacing of 1μm and line averaging 2.
162
163 Ratio-metric calculations for R2D2 auxin sensor were performed using ImageJ (FIJI,
164 https://fiji.sc) as described previously[14]. All the images were processed using IMARIS
165 9.0.0 (bit-plane). Optical sections (transverse or longitudinal) were reconstructed
166 using orthogonal slicer in IMARIS.
167

168

169 **Auxin treatment**

170 Seedlings aged 3DAS were dissected imaged and treated with approximately 10μL of
171 5mM NAA (1-Napthaleneacetic acid) solution in water (0.5M stock in 1M KOH) for
172 60 minutes and imaged again with same settings as prior to treatment.

173

174 **Acknowledgements**

175 We thank Associate Professor Mary Byrne for critical feedback on the manuscript.
176 We thank Dr. Teva Vernoux for kindly providing the seeds of plants expressing
177 *p35S::DII-VENUS* and *p35S::mDII-VENUS* transgenes. We also thank Professor Jim
178 Haseloff for kindly providing the seeds of plants expressing *p35S::H2B-mRFP1* and
179 *p35S::EGFP-LTI6b* transgenes.

180

181 **References**

182 1 Sussex, I. M. Morphogenesis in Solanum tuberosum I: experimental
183 investigation of leaf dorsiventrality and orientation in the juvenile shoot.
184 *Phytomorphology* **5**, 286-300 (1955).
185 2 Reinhardt, D., Frenz, M., Mandel, T. & Kuhlemeier, C. Microsurgical and
186 laser ablation analysis of leaf positioning and dorsoventral patterning in
187 tomato. *Development* **132**, 15-26 (2005).
188 3 Qi, J. *et al.* Auxin depletion from leaf primordia contributes to organ
189 patterning. *Proc Natl Acad Sci U S A* **111**, 18769-18774,
190 doi:10.1073/pnas.1421878112 (2014).
191 4 Brunoud, G. *et al.* A novel sensor to map auxin response and distribution
192 at high spatio-temporal resolution. *Nature* **482**, 103-106,
193 doi:10.1038/nature10791 (2012).
194 5 Vernoux, T. *et al.* The auxin signalling network translates dynamic input
195 into robust patterning at the shoot apex. *Mol Syst Biol* **7**, 508,
196 doi:10.1038/msb.2011.39 (2011).
197 6 Guan, C. *et al.* Spatial Auxin Signaling Controls Leaf Flattening in
198 Arabidopsis. *Curr Biol* **27**, 2940-2950 e2944,
199 doi:10.1016/j.cub.2017.08.042 (2017).
200 7 Qi, J. *et al.* Mechanical regulation of organ asymmetry in leaves. *Nat Plants*
201 **3**, 724-733, doi:10.1038/s41477-017-0008-6 (2017).
202 8 Caggiano, M. P. *et al.* Cell type boundaries organize plant development.
203 *eLife* **6**, doi:10.7554/eLife.27421 (2017).
204 9 Liao, C. Y. *et al.* Reporters for sensitive and quantitative measurement of
205 auxin response. *Nat Methods* **12**, 207-210, 202 p following 210,
206 doi:10.1038/nmeth.3279 (2015).
207 10 Wang, Y. *et al.* The Stem Cell Niche in Leaf Axils Is Established by Auxin
208 and Cytokinin in Arabidopsis. *Plant Cell* **26**, 2055-2067,
209 doi:10.1105/tpc.114.123083 (2014).

11 Federici, F., Dupuy, L., Laplaze, L., Heisler, M. & Haseloff, J. Integrated genetic and computation methods for in planta cytometry. *Nature Methods* **9**, 483-U104, doi:10.1038/nmeth.1940 (2012).

12 Khmelinskii, A. *et al.* Tandem fluorescent protein timers for in vivo analysis of protein dynamics. *Nat Biotechnol* **30**, 708-714, doi:10.1038/nbt.2281 (2012).

13 Barry, J. D., Dona, E., Gilmour, D. & Huber, W. TimerQuant: a modelling approach to tandem fluorescent timer design and data interpretation for measuring protein turnover in embryos. *Development* **143**, 174-179, doi:10.1242/dev.125971 (2016).

14 Bhatia, N. *et al.* Auxin Acts through MONOPTEROS to Regulate Plant Cell Polarity and Pattern Phyllotaxis. *Curr Biol* **26**, 3202-3208, doi:10.1016/j.cub.2016.09.044 (2016).

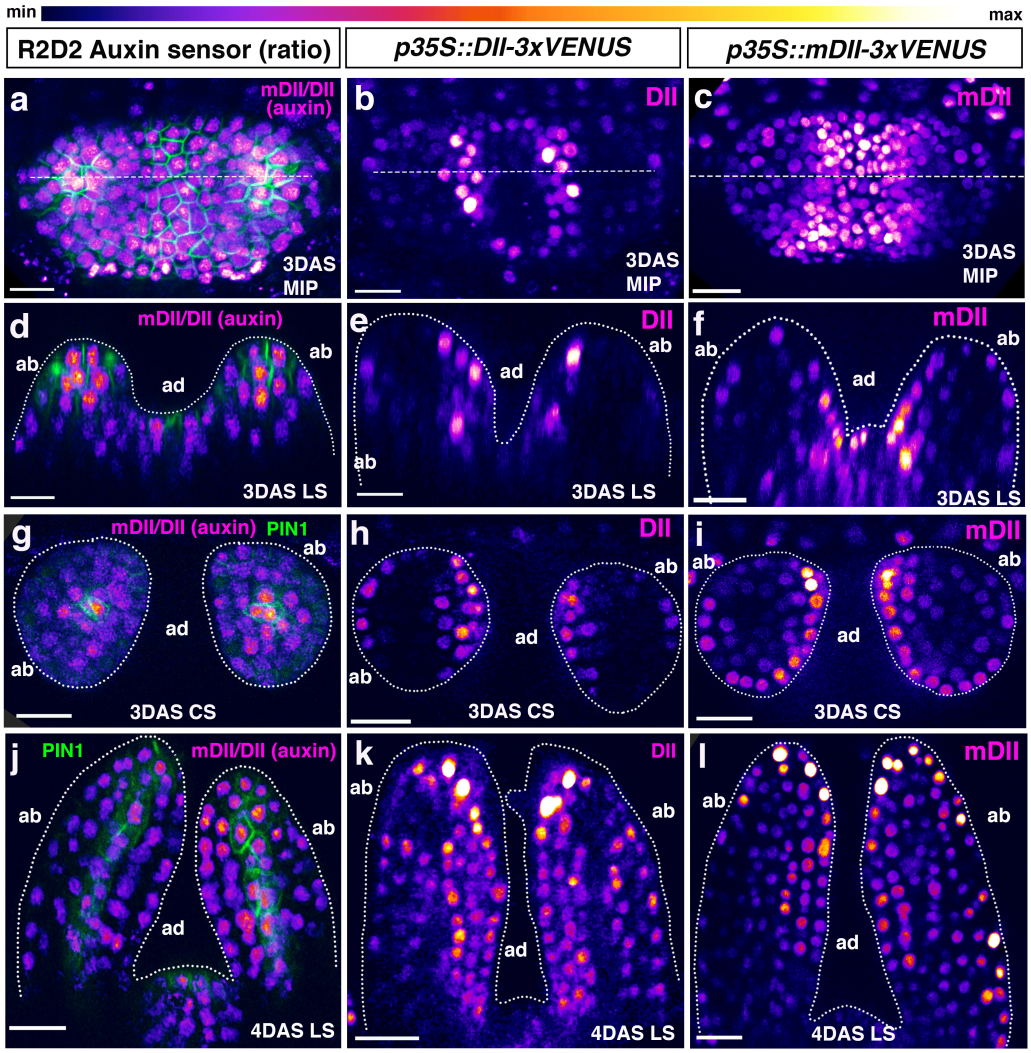


**Figure 1 Predicted auxin distribution in young leaves as indicated by different auxin sensors.**

**(a-c)** Confocal projections of *Arabidopsis* seedlings aged 3DAS (days after stratification) showing predicted auxin distribution based on the ratio-metric auxin sensor R2D2 (magenta) along with PIN1-GFP (green) (a); expression pattern of *p35S::DII-VENUS* (magenta) (b) and *p35S::mutatedDII-VENUS* (mDII, magenta) (c). **(d-f)** Longitudinal reconstructed optical sections of (a-c), respectively, along the dashed lines. **(g-i)** Representative examples of transverse reconstructed optical sections of 3DAS Arabidopsis seedlings showing predicted auxin distribution as indicated by the R2D2 sensor along with PIN1-GFP expression (g), DII-VENUS expression (h) and mDII-VENUS expression (i). R2D2 auxin sensor indicates low but symmetric auxin levels on adaxial and abaxial sides and relatively high auxin levels at the distal tip and in the provasculature where PIN1 expression is also high (d, g). DII-

242 VENUS is more strongly expressed adaxially indicating low auxin levels on the
243 adaxial side of the leaves relative to the abaxial side. However, mDII-VENUS also
244 shows high expression on the adaxial side of the leaf (compare e, h with f, i) and in
245 the shoot meristem. **(j-l)** Representative examples of longitudinal reconstructed
246 optical sections of 4DAS Arabidopsis seedlings showing predicted auxin distribution
247 by R2D2 sensor along with PIN1-GFP expression (green) (i), DII-VENUS expression
248 (j) and mDII-VENUS expression (k). At this stage, the R2D2 sensor indicates a more
249 uniform auxin distribution in the leaf but higher auxin levels in the vasculature where
250 PIN1-GFP expression is also high (j). DII-VENUS shows slightly high expression in
251 adaxial cells and an absence of expression in the vasculature (k). mDII-VENUS
252 shows a similar pattern to DII but is also expressed in the vasculature (l). Scale bars
253 15μm (a-i) and 20μm (j-l).
254

255 FigureS1

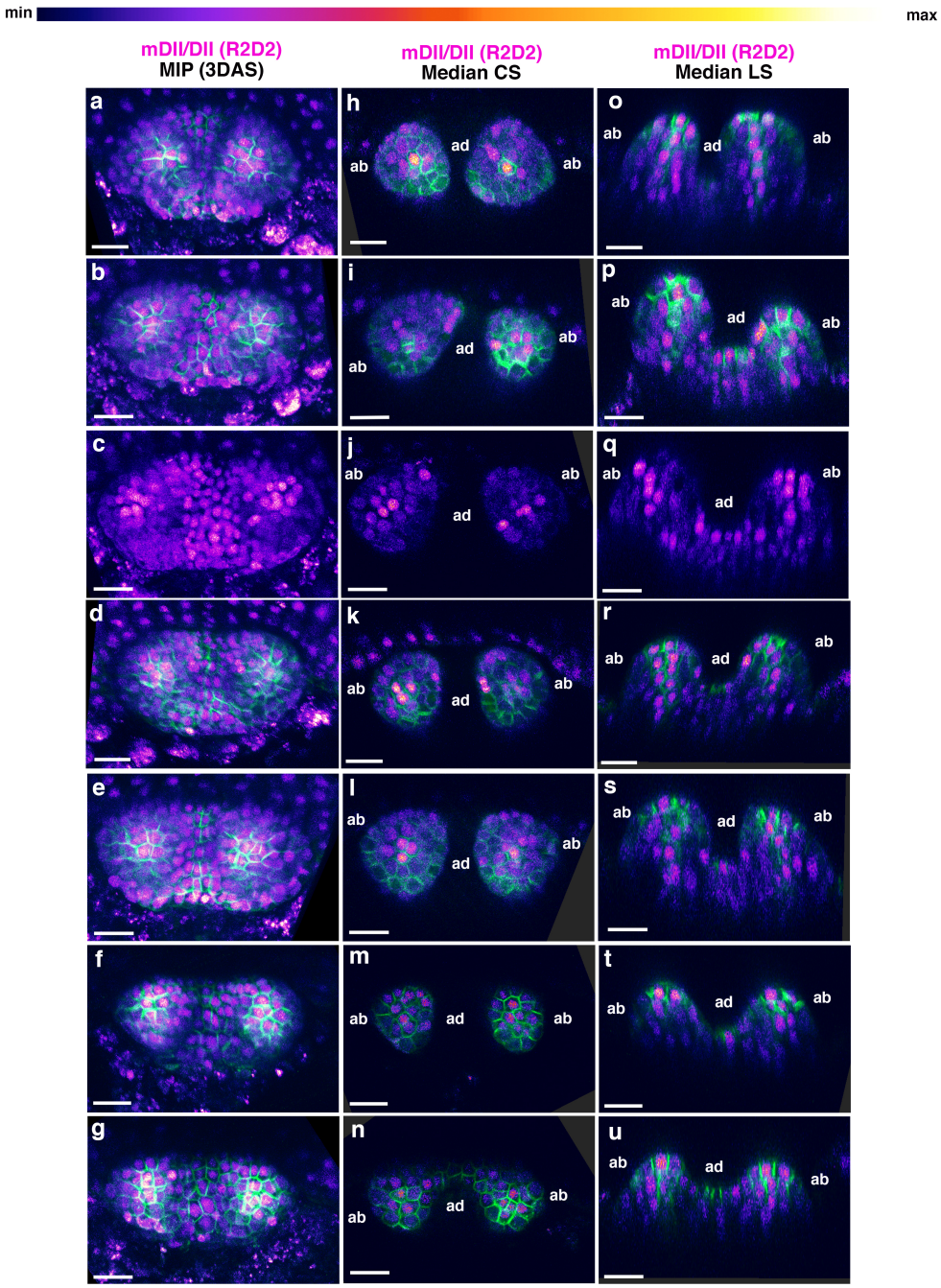


256

257 **FigureS1 Additional examples of R2D2, ratio-based predictions of auxin**
258 **distribution in 3DAS old Arabidopsis seedlings. (a-g)** Confocal projections of
259 *Arabidopsis* seedlings aged 3DAS (days after stratification) showing predicted auxin
260 distribution based on the ratio-metric auxin sensor R2D2 (magenta) along with PIN1-
261 GFP (green). **(h-n)** Median transverse optical sections of (a-g). **(o-u)** Median
262 longitudinal optical sections of (a-g). Scale bars 20μm (a-u).

263

264

265 Figure S2

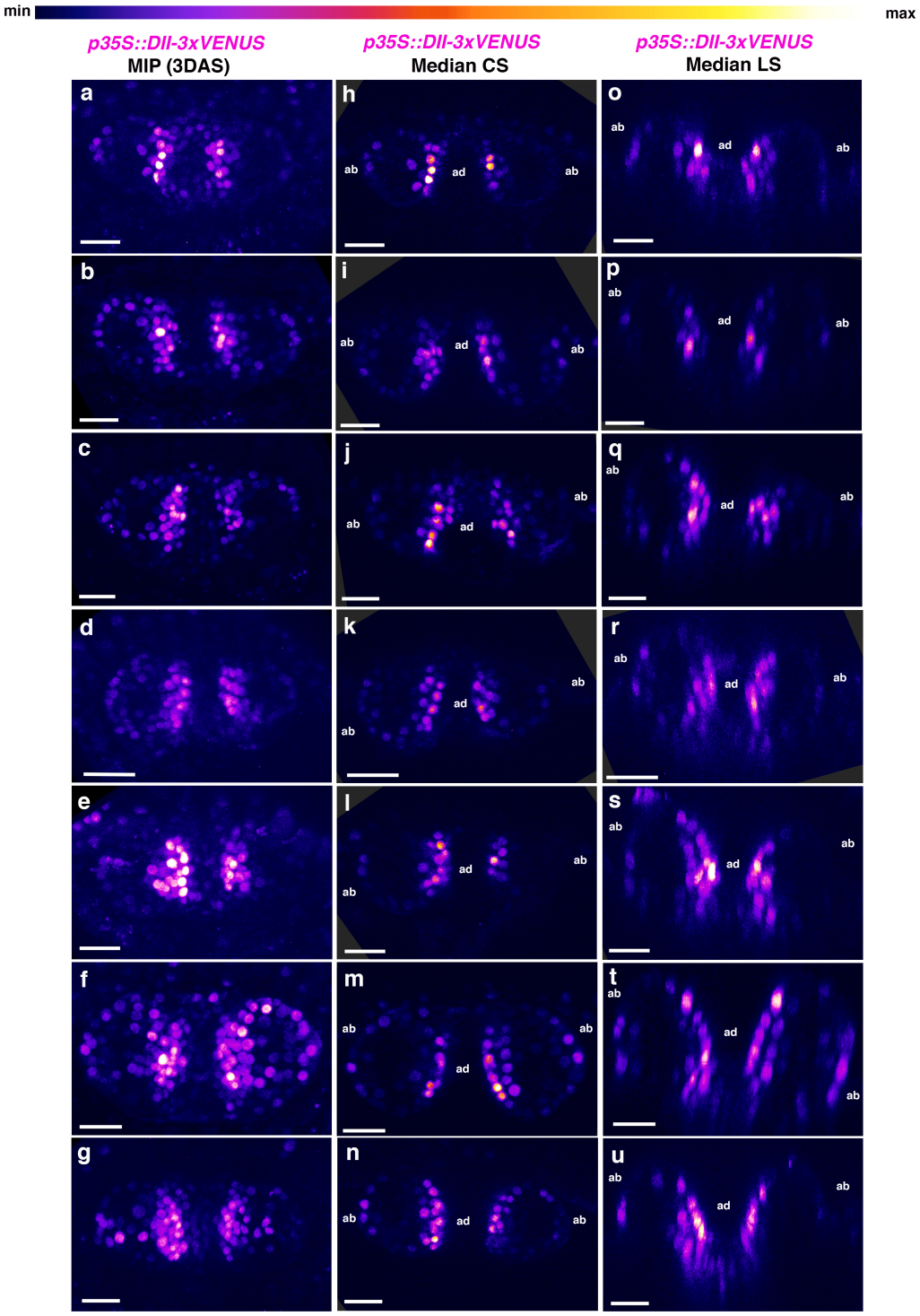


266

267 **FigureS1 Additional examples *p35S::DII-3xVENUS-N7* expression in 3DAS old**
268 **Arabidopsis seedlings. (a-g)** Confocal projections of *Arabidopsis* seedlings aged
269 3DAS (days after stratification) showing expression pattern of p35s::DII-3xVENUS-

N7 sensor (magenta). **(h-n)** Median transverse optical sections of (a-g). **(o-u)** Median longitudinal optical sections of (a-g). Scale bars 20μm (a-u).

272 FigureS3

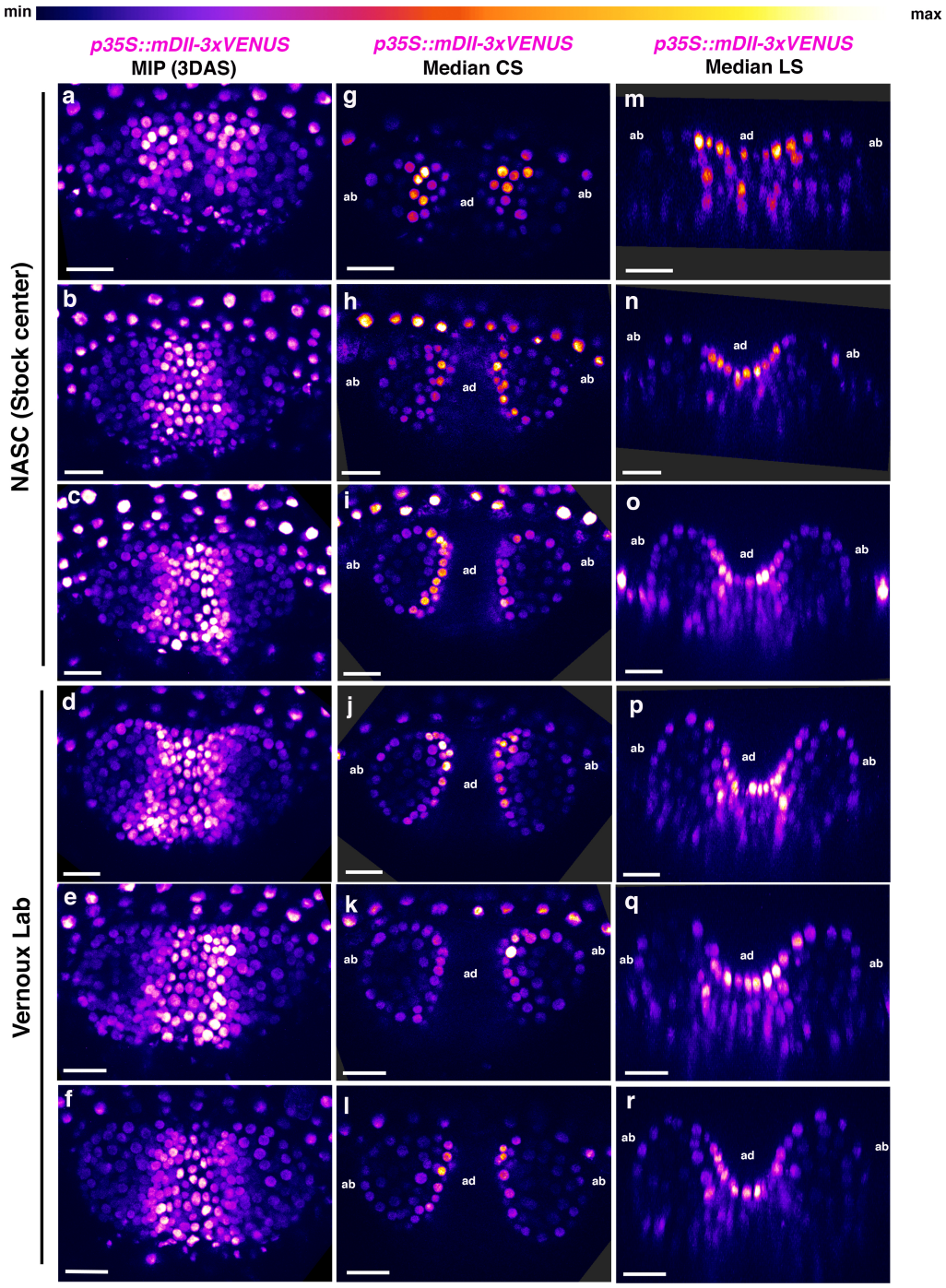


273

274 **FigureS1 Additional examples of *p35S::mDII-3xVENUS-N7* expression in 3DAS**
275 **old Arabidopsis seedlings. (a-f)** Confocal projections of *Arabidopsis* seedlings aged
276 3DAS (days after stratification) showing expression pattern of p35s::mDII-
277 3xVENUS-N7 sensor (magenta). Note that plants obtained from two different sources

showed similar expression pattern. **(h-l)** Median transverse optical sections of (a-f). **(o-r)** Median longitudinal optical sections of (a-g). Scale bars 20μm (a-r).

311 FigureS4

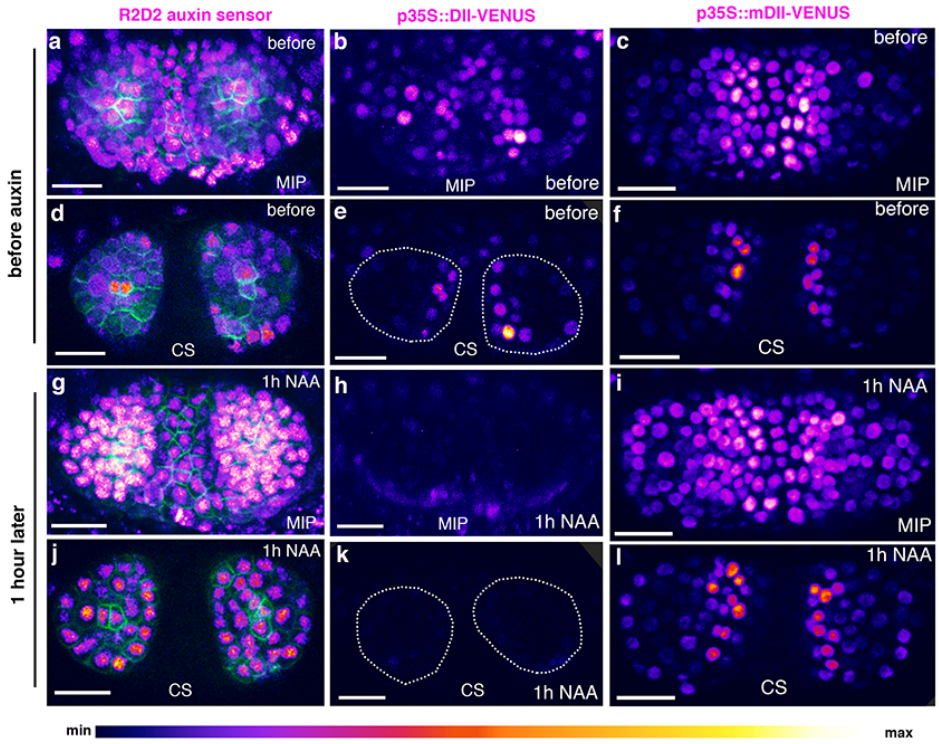


312

313 **Figure S4 Response of different auxin sensors to external auxin application**

314

315 **(a-f)** Confocal projections (a-c) and transverse optical reconstructions (d-f) of
316 *Arabidopsis* seedlings, 3DAS, showing predicted auxin distribution based on R2D2
317 ratio-metric sensor (magenta) along with PIN1-GFP expression in green (a,d), DII-
318 VENUS sensor (magenta) (b,e) and mDII-VENUS sensor (magenta) (c, f) before
319 auxin application. **(g-l)** Confocal projections (g-i) and transverse optical
320 reconstructions (j-l) of *Arabidopsis* seedlings, 3DAS, showing predicted auxin
321 distribution based on R2D2 ratio-metric sensor (magenta) along with PIN1-GFP
322 expression in green (a,d), DII-VENUS sensor (magenta) (b,e) and mDII-VENUS
323 sensor (magenta) (c, f) 1hour after the application of 5mM NAA. Note, R2D2 sensor
324 indicates an increased and broadening of auxin levels after NAA application (compare
325 d and j) (n=3/3). Consistently, DII-VENUS shows an attenuated expression within 1
326 hour of auxin application (compare b,e with h,j) (n=4/4). mDII-VENUS levels do not
327 decrease upon auxin application (compare c,f with i,l) (n=4/4). Scale bars 20μm (a-l).

328

329 Figure S5

330

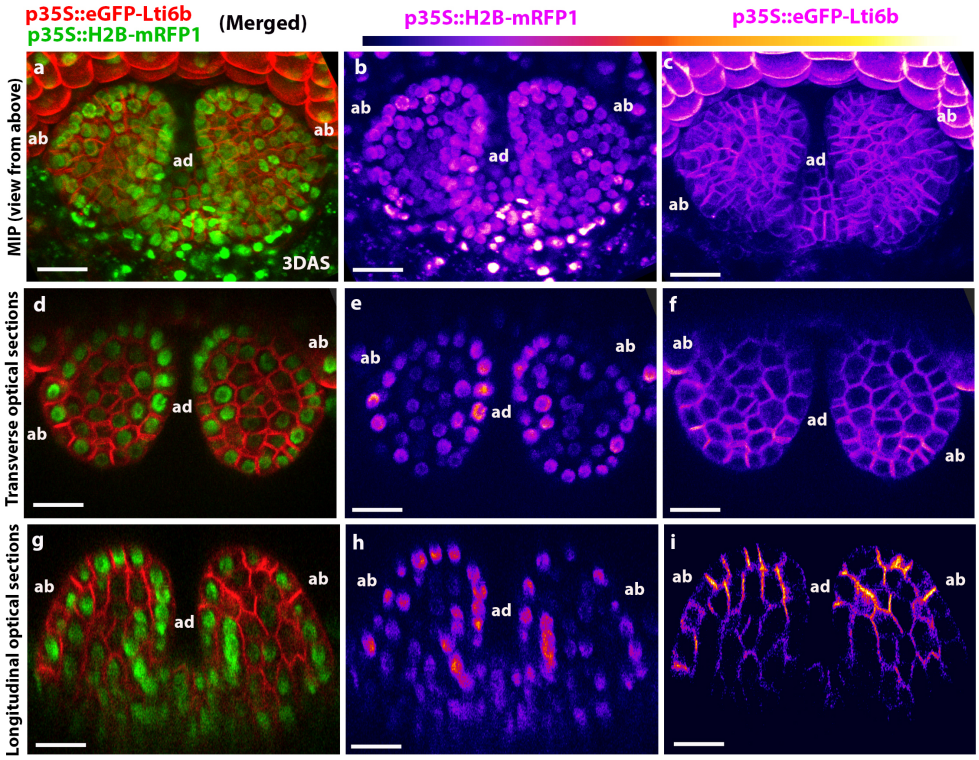


331

332

333 **Figure S5 Different 35S promoter-driven reporter genes show different**
334 **expression patterns in young leaves.**

335

336 **(a-c)** Confocal projections of *Arabidopsis* seedlings aged 3DAS showing expression
337 patterns of a *p35S:eGFP-Lti6b* (membrane marker, green) and *p35S::H2B-*
338 *mRFP1*(nuclear marker red) together (a), *p35S::H2B-mRFP1* only (magenta) (b) and
339 *p35S:eGFP-Lti6b* only (magenta) (c). **(d-f)** Transverse optical reconstructions of (a-c)
340 respectively; merged (d), *p35S::H2B-mRFP1* only (magenta) (e) and *p35S:eGFP-*
341 *Lti6b* only (magenta) (f). **(g-i)** Longitudinal optical reconstruction of (a-c)
342 respectively; merged (g), *p35S::H2B-mRFP1* only (magenta) (h) and *p35S:eGFP-*
343 *Lti6b* only (magenta) (i). Note *p35S::H2B-mRFP1* shows similarly high levels of
344 expression in both adaxial (ad) as well as abaxial (ab) epidermal cell layers and
345 weaker expression in the middle regions (e and h). However, *p35S:eGFP-Lti6b* shows
346 no consistent asymmetry in expression throughout the leaf (f and i). Scale bars 20μm
347 (a-i), (n=10 leaves).

348